PHASE-FIELD APPROACH TO CRYSTAL GROWTH

HUNG HOANG DIEU[1] , MICHAL BENEŠ[1] , AND ATSUSHI SUZUKI[2]

Abstract. The phase-field method has appeared in the context of diffuse interfaces. It has been applied to the three major materials processes: solidification, solid-state phase transformation, and grain growth and coarsening. Very recently, a number of new phase-field models have been developed for modelling thin films and surfaces (see [3]). The first part of this contribution is concerned with the phase-field model of spiral crystal growth [5] described by the Burton-Cabrera-Frank theory [2]. We then present computational studies related to the pattern formation and to the dependence on model parameters. The second part is concerned with the phase-field model [4, 6] of heteroepitaxial growth. Finally, we present our latest results.

Key words. phase field model, spiral growth, heteroepitaxial growth, FDM, FEM

AMS subject classifications. 35K55, 35R35, 80A20, 80M40

1. Spiral Crystal Growth. Classically epitaxial crystal growth is modelled using Burton-Cabrera-Frank (BCF) theory [2]. According to that theory, atoms are first adsorbed to the crystalline surface. Such atoms are called adatoms. They then diffuse freely along the surface and they can either desorb from the surface with a probability $1/\tau_S$ per unit time, or they are incorporated into the crystal at one of the three sites: ledge site, step site or kink site. Incorporation at a kink site will be the most energetically favourable.
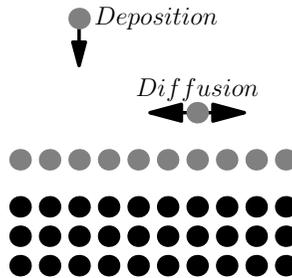

Fig. 1.1: Atomistic view of the basic processes in epitaxy.

The basic equations in the phase-field formulation of BCF model [2, 5] are

$$\partial_t c = D\Delta c - \frac{c}{\tau_S} + F - \Omega^{-1}\partial_t \Phi, \tag{1.1}$$

$$\alpha\partial_t \Phi = \xi^2 \Delta \Phi + sin(2\pi(\Phi - \Phi_S)) + \lambda c(1 + cos(2\pi(\Phi - \Phi_S))), \tag{1.2}$$

where c is the adatom density, D is the surface diffusion coefficient, τ_S is the mean time for the desorption of adatoms from the surface, F is the deposition rate, Ω is

---

[1]Department of Mathematics, Faculty of Nuclear Sciences and Physical Engineering, Czech Technical University in Prague, Czech Republic.

[2]Laboratoire Jacques-Louis Lions, Universit Pierre et Marie Curie, France.

the atomic area, Φ is the surface height in units of atoms, α is the time relaxation parameter, ξ is the width of steps between terraces, Φ_S is the height of the initial substrate surface and λ is the coupling constant.

The boundary conditions are given by

$$\frac{\partial c}{\partial n}(t, \mathbf{x}) = \frac{\partial \Phi}{\partial n}(t, \mathbf{x}) = 0, t \in (0, T). \tag{1.3}$$

The initial conditions are given by

$$c(0, \mathbf{x}) = 0, \tag{1.4}$$

$$\Phi(0, \mathbf{x}) = \Phi_S(\mathbf{x}). \tag{1.5}$$

1.1. Numerical Scheme. We use an explicit scheme of the finite difference method to solve the free boundary problem of spiral crystal growth. The first step in the discretization is to divide the computational domain into a two-dimensional grid and then derivatives are replaced with equivalent finite differences.

We consider the computational domain S to be a rectangle $(0, L_1) \times (0, L_2)$ which is to be discretized. We partition the domain S using a grid of internal nodes $\omega_h = \{(ih_1, jh_2)|i = 1, ..., N_1 - 1, j = 1, ..., N_2 - 1\}$, where $h_1 = \frac{L_1}{N_1}, h_2 = \frac{L_2}{N_2}$ are the mesh sizes in S. We discretize the time interval using a mesh $[0, T] : T_\tau = \{k\tau | k = 0, ..., N_T\}$, where $\tau = \frac{T}{N_T}$ is a time step. Then we can consider a grid function $u : T_\tau \times \omega_h \to \mathbb{R}$ for which $u_{ij}^k = u(ih_1, jh_2, k\tau)$.

The time derivative is approximated by forward difference

$$\partial_t u_{ij}^k \approx \frac{u_{ij}^{k+1} - u_{ij}^k}{\tau},$$

and the space derivatives are approximated by second-order central differences:

$$\partial_{xx} u_{ij}^k \approx \frac{u_{i+1,j}^k - 2u_{ij}^k + u_{i-1,j}^k}{h_1^2},$$

$$\partial_{yy} u_{ij}^k \approx \frac{u_{i,j+1}^k - 2u_{ij}^k + u_{i,j-1}^k}{h_2^2}.$$

Then the discrete Laplace operator in two dimensions is given by

$$\Delta_h u^k{}_{ij} = \frac{u_{i+1,j}^k - 2u_{ij}^k + u_{i-1,j}^k}{h_1^2} + \frac{u_{i,j+1}^k - 2u_{ij}^k + u_{i,j-1}^k}{h_2^2}.$$

The explicit scheme has the form

$$\alpha \frac{\Phi_{ij}^{k+1} - \Phi_{ij}^k}{\tau} = \xi^2 \Delta_h \Phi_{ij}^k + sin(2\pi(\Phi_{ij}^k - \Phi_{S_{ij}}^k))$$
$$+ \lambda c_{ij}^k(1 + cos(2\pi(\Phi_{ij}^k - \Phi_{S_{ij}}^k))), \tag{1.6}$$

$$\frac{c_{ij}^{k+1} - c_{ij}^k}{\tau} = D\Delta_h c_{ij}^k - \frac{c_{ij}^k}{\tau_S} + F - \Omega^{-1} \frac{\Phi_{ij}^{k+1} - \Phi_{ij}^k}{\tau} \tag{1.7}$$

for $i = 1, ..., N_1 - 1, j = 1, ..., N_2 - 1, k = 0, ..., N_T$.

Discretization of the spiral crystal growth problem leads to a system of equations

$$\Phi_{ij}^{k+1} = \Phi_{ij}^{k} + \frac{\tau \xi^2}{\alpha} \frac{\Phi_{i+1,j}^{k} + \Phi_{i,j+1}^{k} - 4\Phi_{ij}^{k} + \Phi_{i,j-1}^{k} + \Phi_{i-1,j}^{k}}{h^2}$$

$$+ \frac{\tau}{\alpha} sin(2\pi(\Phi_{ij}^{k} - \Phi_{S_{ij}}^{k}))$$

$$+ \frac{\tau \lambda}{\alpha} c_{ij}^{k}(1 + cos(2\pi(\Phi_{ij}^{k} - \Phi_{S_{ij}}^{k}))), \tag{1.8}$$

$$c_{ij}^{k+1} = c_{ij}^{k} + \tau D \frac{c_{i+1,j}^{k} + c_{i,j+1}^{k} - 4c_{ij}^{k} + c_{i,j-1}^{k} + c_{i-1,j}^{k}}{h^2}$$

$$- \frac{\tau}{\tau_S} c_{ij}^{k} + \tau F - \frac{\Phi_{ij}^{k+1} - \Phi_{ij}^{k}}{\Omega} \tag{1.9}$$

for $i = 1, ..., N_1 - 1, j = 1, ..., N_2 - 1, k = 0, ..., N_T$. That means we can obtain the values at time $k + 1$ from the corresponding ones at time k.

For $h = h_1 = h_2$, we expect this explicit method is numerically stable and convergent whenever $\frac{\xi^2 \tau}{\alpha h^2} \leq \frac{1}{4}$ and $\tau(\frac{4D}{h^2} + \frac{1}{\tau_S}) \leq 1$.

The boundary conditions are treated by mirroring the values in the inner nodes across the boundary.
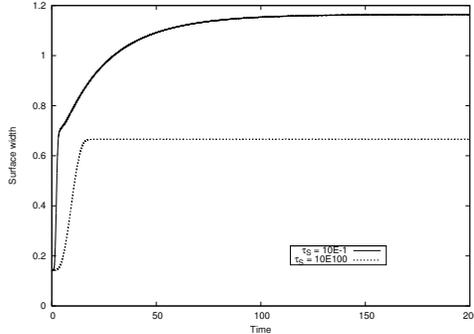

Fig. 1.2: Comparison of transient dynamics for different desorption times. Top line: the surface width changes slowly in time. Bottom line: the surface width quickly levels off and remains constant.

1.2. Numerical Results. The purpose of this section is to show the relation between the model parameter τ_S and growth pattern. The other parameters are set up as follows: $\Omega = 2.0$, $\alpha = 1.0$, $\xi = 1.0$, $\lambda = 10.0$, $D_S = 2.0$, $F = 3.0$, $\tau = 0.00025$, $N_T = 100000$, so that $T = 25$. The dimensions of ω_h are 100×100, the spatial step size is set to $50/99$, and $L = 50$. The initial height of the substrate Φ_S is formed by $\frac{arctan(y/x)}{2\pi}$ for the dislocation. First, transient dynamics (see Fig. 1.2) is quantified by defining the so called surface width $w(t)$ which represents the mean fluctuation of the surface height

$$w(t) = \frac{1}{2}\langle \Phi(x,t)^2 - \langle \Phi(x,t)\rangle^2\rangle^{1/2},$$
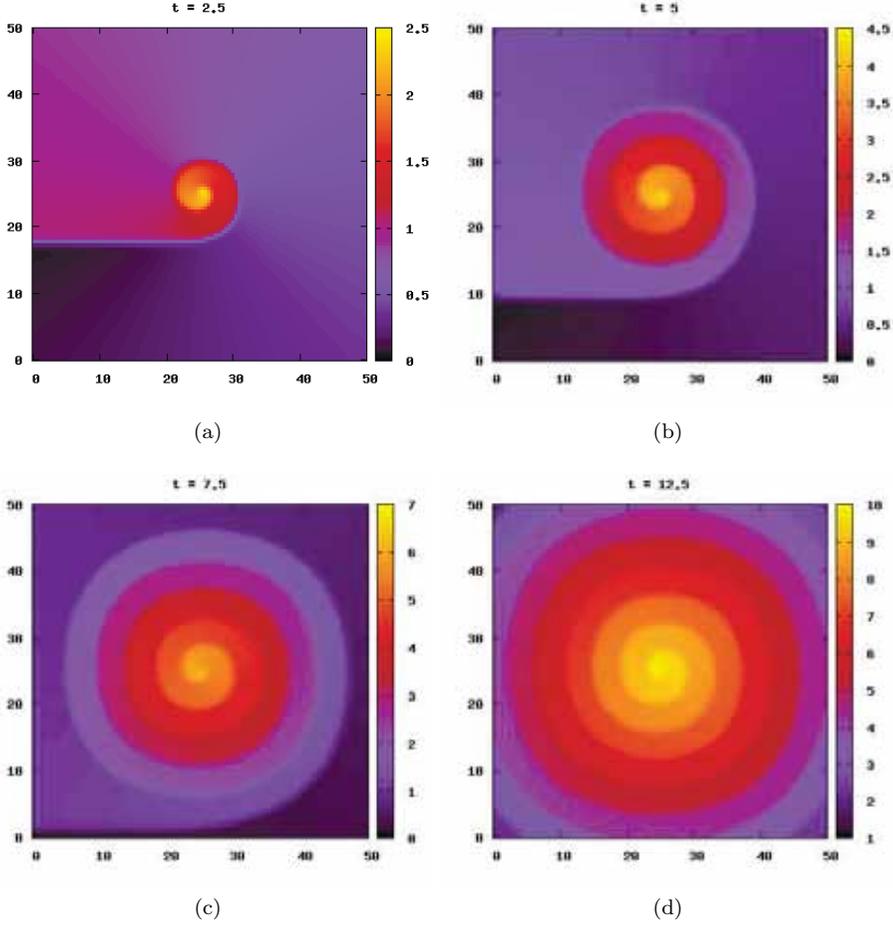
where $\langle f \rangle = L^{-2} \int_S f dx$.

Fig. 1.3: Spiral ridge at different times t for $\tau_S = 0.1$. Colour palette represents the surface height.

In the numerical experiments, we observed two distinguished growth regimes. As can be seen in Fig. 1.3 for small τ_S, the spiral finds its final step spacing l essentially after a single rotation. In contrast, for very large τ_S the transient spiral ridge evolves slowly towards a spiral with a constant l. This surface evolution is demonstrated in Fig. 1.4.

2. Heteroepitaxial Growth. Epitaxy refers to the oriented growth of crystalline material onto the single crystal surface. The orientation is determined by the underlying crystal. In general, we distinguish two cases:

- Homoepitaxy – the growth layers of the material and the substrate are of the same chemical composition.
- Heteroepitaxy – the growth layers of the material and the substrate are of the different chemical compositions.

Our aim is to study heteroepitaxial growth which is under misfit stress. This leads to morphological instability (known as the Asaro-Tiller-Grinfeld instability [1]).
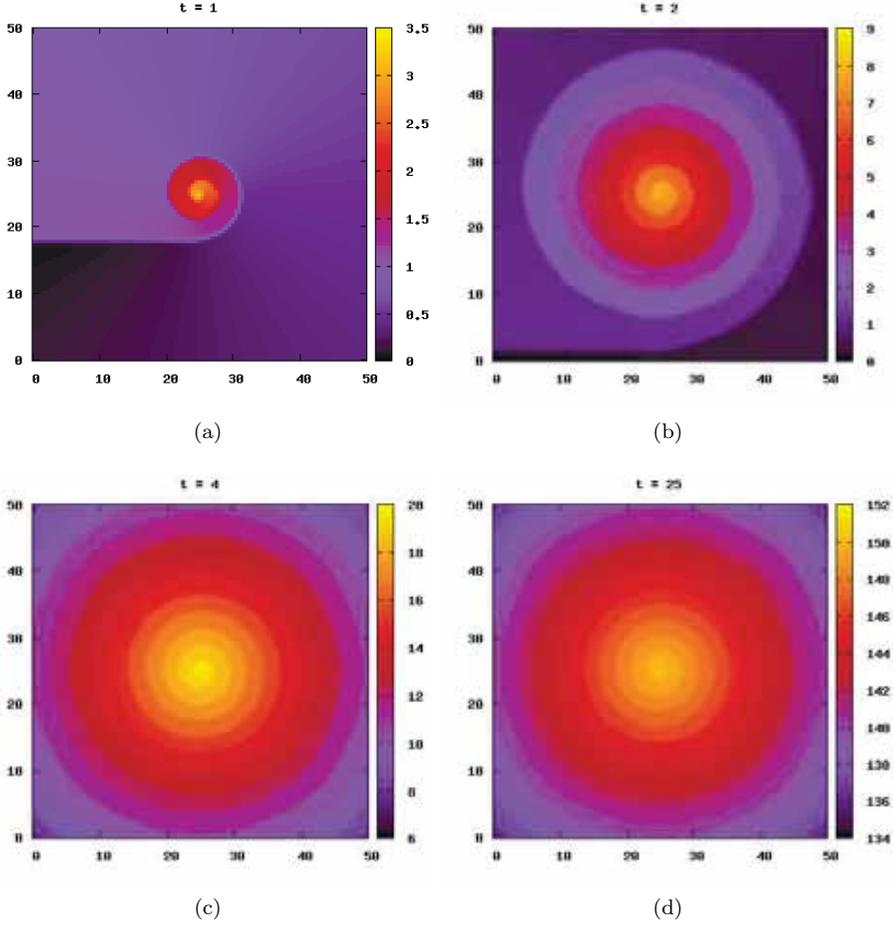
Fig. 1.4: Spiral ridge at different times t for large τ_S. Colour palette represents the surface height.

We consider a system Ω consisting of two regions – a solid epitaxial film $\Omega^e(t)$ and vapour phase $\Omega^v(t)$. The solid-vapour interface is denoted $\Gamma(t)$, which is a function of time t (see Fig. 2.1). We introduce an extensive scalar quantity Φ, called the phase-field,

$$
\Phi(t, \mathbf{x}) \begin{cases} = 0 & \mathbf{x} \in \Omega^v \\ = 1 & \mathbf{x} \in \Omega^e \\ \in (0,1) & \mathbf{x} \in \Gamma(t) \end{cases}.
$$

This quantity takes a value $\Phi = 0$ in the vapour and $\Phi = 1$ in the solid. It varies rapidly in the interface.

Here, the linear elastic theory is used. The stress tensor $\sigma_{ij}^{(v)}$ in the vapour is given by Hooke's law

$$
\sigma_{ij}^{(v)} = 2\mu^{(v)}\epsilon_{ij} + \lambda^{(v)}\epsilon_{kk}\delta_{ij},
$$

where Einstein summation convention is implied.

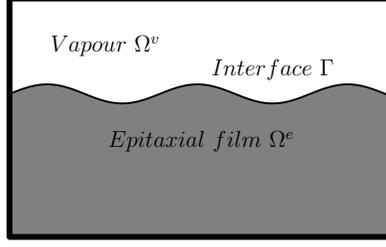Following [8] the stress tensor $\sigma_{ij}^{(e)}$ in the epitaxial film is given by

Fig. 2.1: Model.

$$\sigma_{ij}^{(e)} = 2\mu^{(e)}\epsilon_{ij} + \lambda^{(e)}\epsilon_{kk}\delta_{ij} - \epsilon^m\{\tfrac{1+\nu^{(e)}}{1-2\nu^{(e)}}\}\delta_{ij}.$$

$\mu^{(*)}, \lambda^{(*)}$ are the Lamé constants, $\nu^{(*)}$ is the Poisson's ratio, where $* \in \{e, v\}$. $\epsilon^m = \frac{a_e - a_s}{a_s}$ is the misfit strain, where a_e, a_s are lattice constants of epitaxial film or substrate. The strain tensor is given by $\epsilon_{ij} = \frac{1}{2}\left(\frac{\partial u_i}{\partial x_j} + \frac{\partial u_j}{\partial x_i}\right)$, where u_i is the ith component of the displacement vector.

The stress tensor in the system is determined from

$$0 = \frac{\partial}{\partial x_j}\{h(\Phi)\sigma_{ij}^{(e)} - [1 - h(\Phi)]\sigma_{ij}^{(v)}\}, \tag{2.1}$$

where $h(\Phi) = \Phi^2(3 - 2\Phi)$ is the weight function for the epitaxial layer (see [6]).

The equation of motion is

$$\xi\partial_t\Phi = A\xi\Delta\Phi + \frac{B}{\xi}g'(\Phi)$$
$$+ Ch'(\Phi)\{(\mu^{(e)} - \mu^{(v)})\epsilon_{ij}\epsilon_{ij} + \frac{\lambda^{(e)} - \lambda^{(v)}}{2}(\epsilon_{ii})^2 \tag{2.2}$$
$$- \frac{1 + \nu^{(e)}}{1 - 2\nu^{(e)}}(\epsilon^m)^2\},$$

where ξ is the width of the transition region, A, B, C are constants, $g'(\Phi) = 2\Phi(1 - \Phi)(1 - 2\Phi)$, and $h'(\Phi) = 6\Phi(1 - \Phi)$.

2.1. Numerical Results. We implemented the model using the explicit scheme based on finite difference method for the phase-field equation (2.2). In the numerical experiments, we used the rectangular domain $\Omega \equiv (0, 2) \times (0, 1)$ with the grid 200×100. The spatial step size in x-direction is set to $h_1 = 2/199$ and the spatial step size in y-direction is set to $h_2 = 1/99$. The other model parameters are as follows: $A = 0.005$, $B = -0.01$, $C = -0.00333$, $\xi = 0.015$, and time step $\tau = A * h_1 * h_1/8$. The initial conditions for the phase-field variable are given by

$$\Phi(x, y) = 0.5\left(tanh\left(\frac{1}{h_1}(0.1cos(3\pi x) - y)\right) + 1\right).$$

For the elastic problem, we used FreeFem++ [7] based on FEM. Material dimensionless parameters are taken as follows: $E^{(v)} = 1$, $\nu^{(v)} = 0$, $E^{(e)} = 1 \times 10^7$, $\nu^{(v)} = 0.278$, $\epsilon^m = 0.05$, $\mu = E/(2.0(1.0 + \nu))$, $\lambda = E\nu/((1.0 + \nu)(1.0 - 2.0 * \nu))$. Computations of stress field were very time consuming. Fig. 2.2b shows x-component

of normal strain at t = 0.00038. Here, we can see that misfit stress relaxes at the tops of islands.

Finally, Fig. 2.2a displays the evolution of the interface. We observe the valleys of the surface profile deepen under stress. However, the tops deepen as well, even at higher speed.
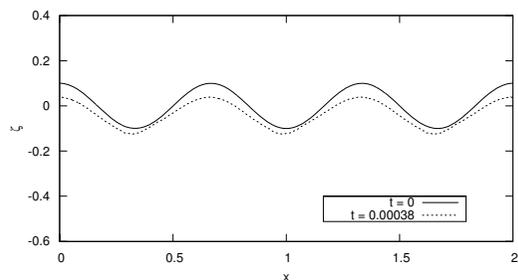
(a) Evolution of the interface. ζ is the interface position, given by its z coordinate.
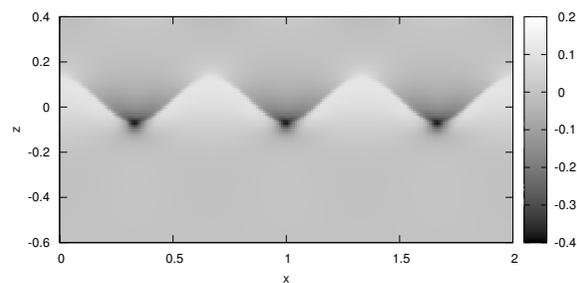
(b) Normal strain in x-direction at $t = 0.00038$.

Fig. 2.2: Numerical results.

3. Conclusion. Our major conclusions are as follows. In the context of spiral growth, we conclude that step spacing is dependent on desorption time. The larger desorption time is, the smaller the step spacing is. In the second part of the contribution, the phase-field model for heteroepitaxial growth seems to describe the nature of the ATG instability. However, our study is at early stage and it is not obvious from the experiments whether it can lead to fracture or it evolves towards the planar interface. We also found that numerical noise avoid us to simulate the problem in longer time. Therefore, it is necessary to develop better numerical schemes suitable for modelling heteroepitaxial growth.

REFERENCES

[1] R. Asaro and W. Tiller, *Interface morphology development during stress corrosion cracking: Part i. via surface diffusion*, Metallurgical and Materials Transactions B **3** (1972), 1789–1796. 10.1007/BF02642562.

[2] W. K. Burton, N. Cabrera, and F. C. Frank, *The growth of crystals and the equilibrium structure of their surfaces*, Phil. Trans. R. Soc. **243** (1951), 299–358.

[3] L. Q. Chen, *Phase-field models for microstructure evolution*, Annual Review of Materials Research, **32** (2002), 113–140.

[4] H. Emmerich, *The diffuse interface approach in materials science: thermodynamic concepts and applications of phase-field models*, Lecture notes in physics: Monographs, Springer-Verlag (2003).

[5] A. Karma and M. Plapp, *Spiral Surface Growth without Desorption*, Phys. Rev. Lett., **81** (1998), 4444–4447.

[6] K. Kassner, C. Misbah, J. Müller, J. Kappey, and P. Kohlert, *Phase-field modeling of stress-induced instabilities*, Phys. Rev. E **63** (2001), 036117.

[7] O. Pironneau, F. Hecht, A. L. Hyaric, and J. Morice, *Freefem++*. http://www.freefem.org/ff++/.

[8] B. J. Spencer, P. W. Voorhees, and S. H. Davis, *Morphological instability in epitaxially strained dislocation-free solid films*, Phys. Rev. Lett. **67** (1991), 3696–3699.